OMTN, Volume *28*

Supplemental information

RPS4XL encoded by lnc-Rps4l inhibits hypoxia-induced pyroptosis by binding HSC70 glycosylation site

Yiying Li, Junting Zhang, Hanliang Sun, Xiufeng Yu, Yujie Chen, Cui Ma, Xiaodong Zheng, Lixin Zhang, Xijuan Zhao, Yuan Jiang, Wei Xin, Shanshan Wang, Jiye Hu, Mingge Wang, and Daling Zhu

Supplemental Figures

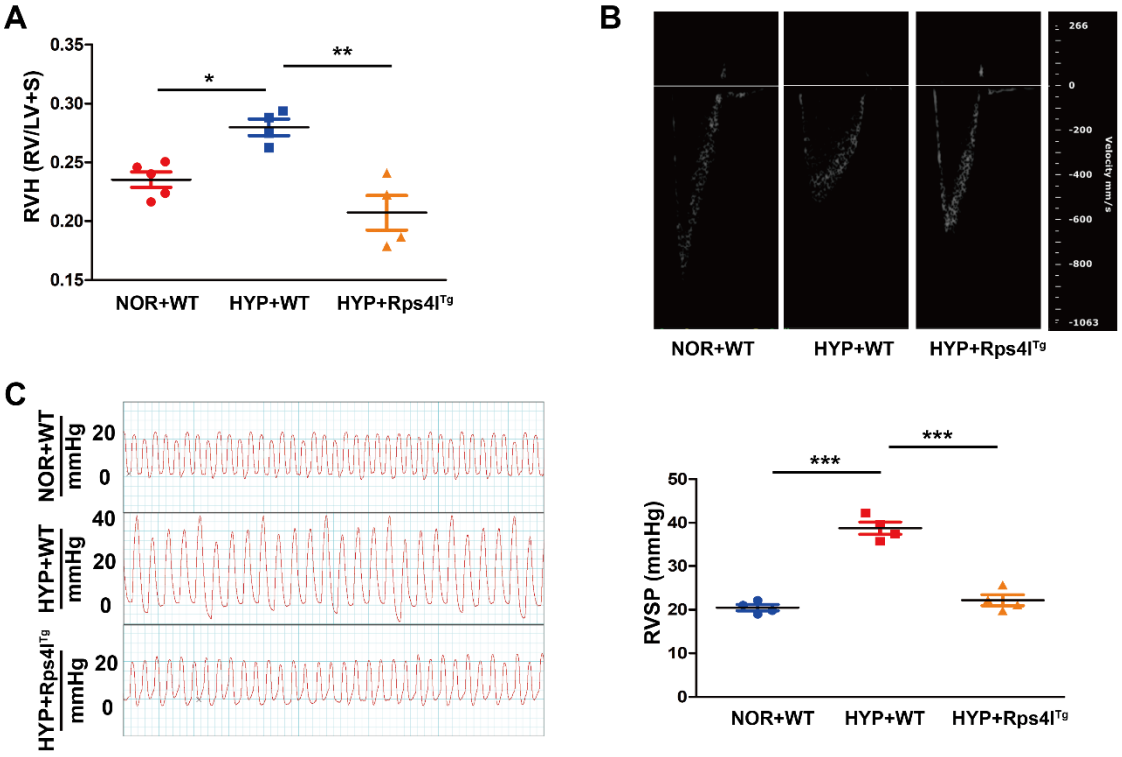

Supplemental Figure 1. Establishment of a hypoxia model in lnc-Rps4l-overexpressing transgenic mice. (A) RV/(LV+S) of Rps4lTg and WT hypoxic and normoxic mice. (B) Echocardiographic images of Rps4lTg and WT hypoxic and normoxic mice. (C) Right ventricular systolic pressure (RVSP) of Rps4lTg and WT hypoxic and normoxic mice. All values are represented as the mean ± SEM (*$p<0.05$, **$p<0.01$, and ***$p< 0.001$; $n \geq 3$). WT, wild type; NOR, normoxia; HYP, hypoxia.

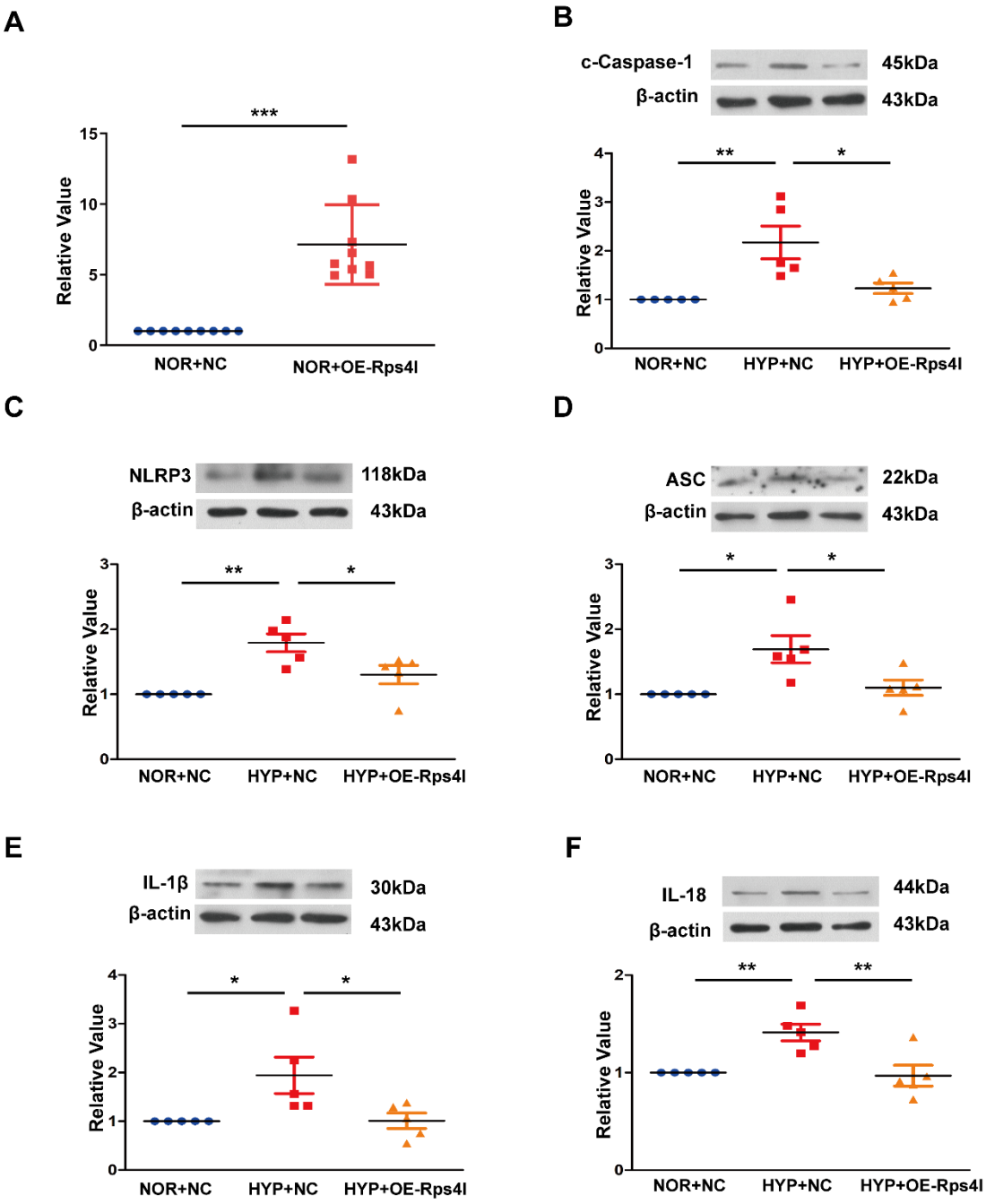

Supplemental Figure 2. (A) Overexpression efficiency of lnc-Rps4l. (B–F) Western blotting analysis of (B) c-caspase-1, (C) NLRP3, (D) ASC, (E) IL-1β, and (F) IL-18 in hypoxic and normoxic PASMCs transfected with OE-Rps4l or OE-NC. All values are represented as the mean ± SEM (*p<0.05, **p<0.01, and ***p< 0.001; n ≥ 3). NOR, normoxia; HYP, hypoxia. All values are represented as the mean ± SEM (*p<0.05, **p<0.01, and ***p< 0.001; n ≥ 3). NOR, normoxia; HYP, hypoxia.

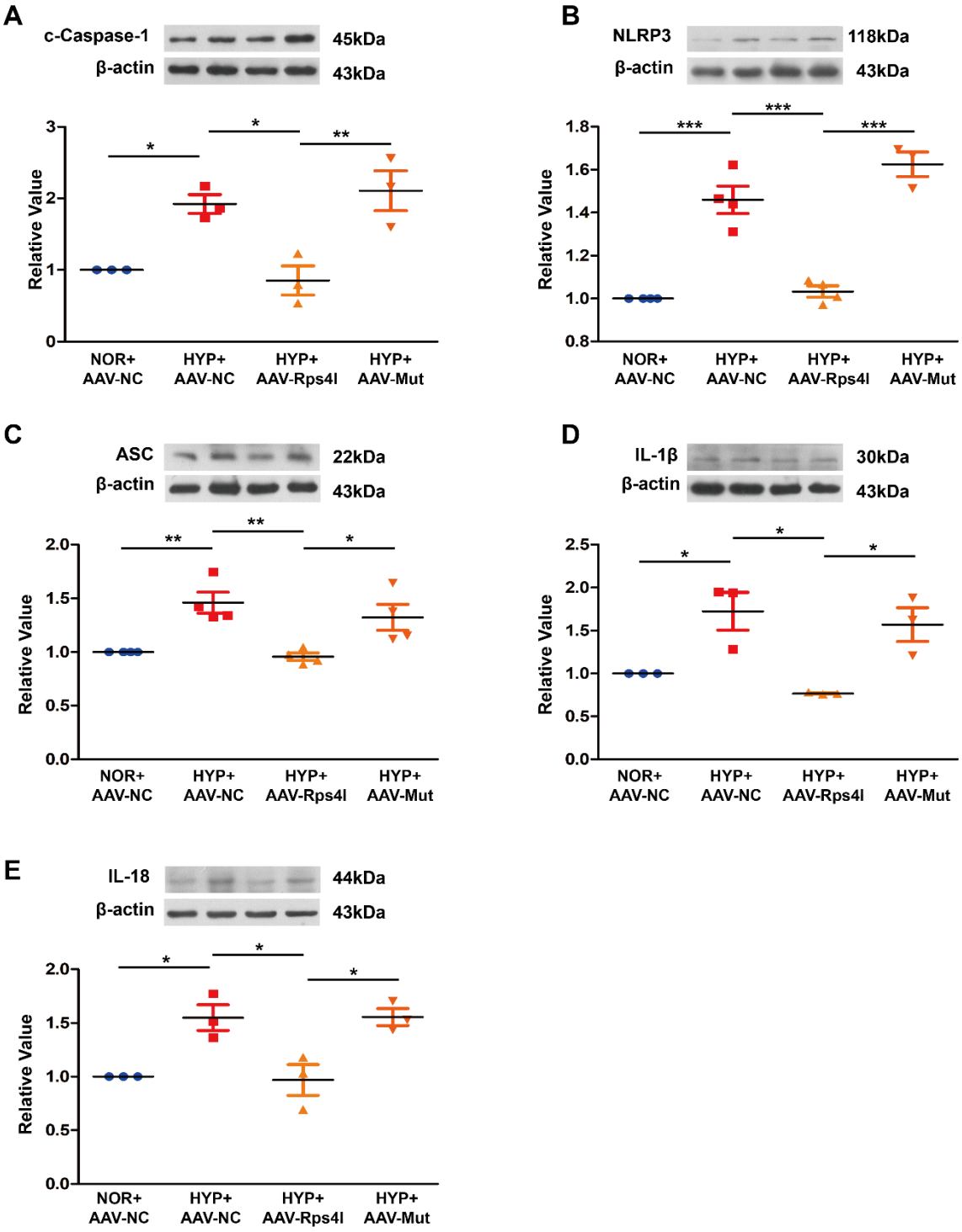

Supplemental Figure 3. lnc-Rps4l-encoded peptide RPS4XL attenuates hypoxia-induced pyroptosis *in vivo*. (A–E) Protein expression analysis of (A) c-caspase-1, (B) NLRP3, (C) ASC, (D) IL-1β, and (E) IL-18 in the lung tissues of hypoxic mice infected with AAV9-NC, AAV9-Rps4l, and AAV9-mut. All values are represented as

the mean ± SEM (*p<0.05, **p<0.01, and ***p< 0.001; n ≥ 3). NOR, normoxia; HYP, hypoxia.

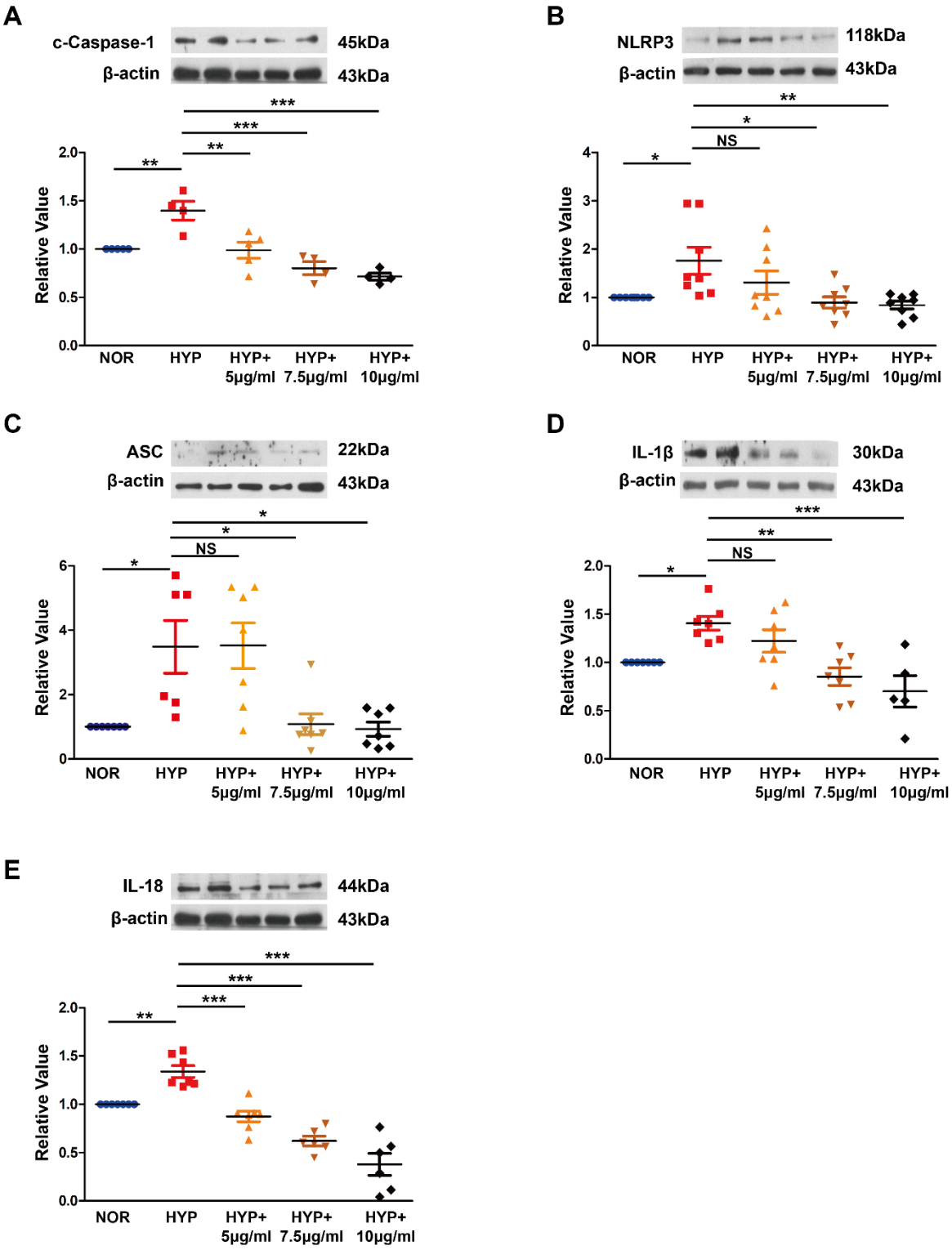

Supplemental figure 4. Exogenous RPS4XL inhibits hypoxia-induced pyroptosis in human PASMCs. (A–E) Western blotting analysis of (A) c-caspase-1, (B) NLRP3, (C) ASC, (D) IL-1β, and (E) IL-18 in human PASMCs treated with 5 μg/ml, 7.5 μg/ml, or 10 μg/ml RPS4XL under hypoxic conditions. All values are represented

as the mean ± SEM (*p<0.05, ** p<0.01, and ***p<0.001; n ≥ 3). NOR, normoxia; HYP, hypoxia; NS, no significance.

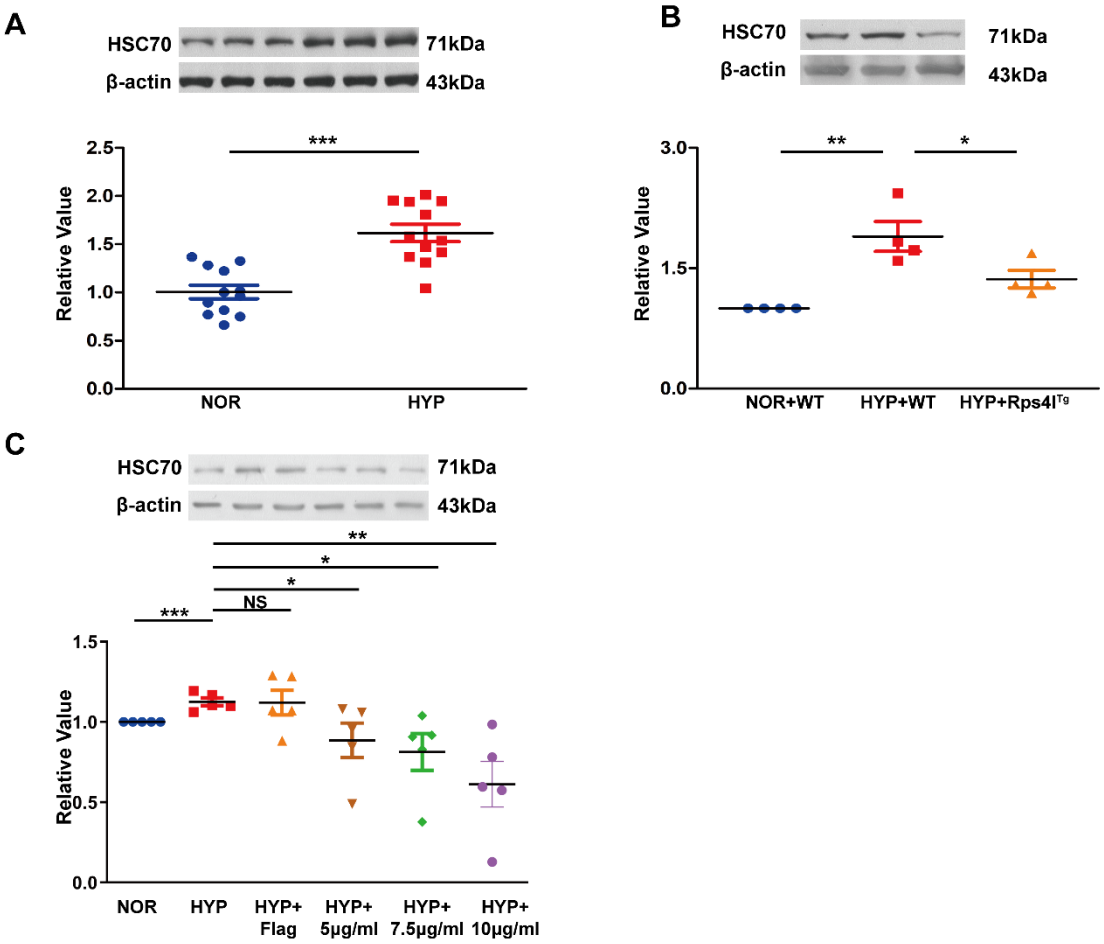

Supplemental figure 5. HSC70 is up-regulated under hypoxic conditions. (A) Western blotting analysis of HSC70 in hypoxic and normoxic PASMCs. (B) HSC70 protein expression in the lung tissues of Rps4lTg and WT hypoxic and normoxic mice. (C) Western blotting analysis of HSC70 in PASMCs treated with 5 μg/ml, 7.5 μg/ml, or 10 μg/ml RPS4XL under hypoxic conditions. Flag was used as a negative control. All values are represented as the mean ± SEM (*p<0.05, **p<0.01, and ***p< 0.001; n ≥ 3). WT, wild type; NOR, normoxia; HYP, hypoxia.

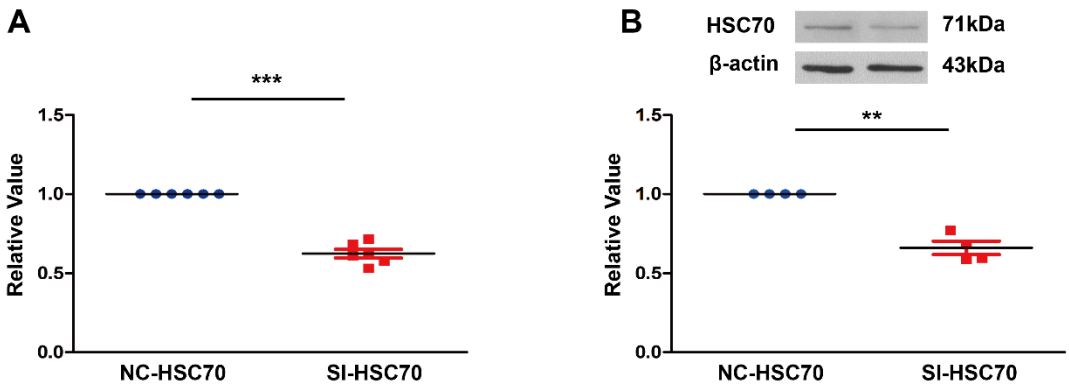

Supplemental Figure 6. Interference efficiency of HSC70 RNAi in PASMCs. (A) Interference efficiency of *HSC70* mRNA levels. (B) Interference efficiency of HSC70 at the protein level. All values are represented as the mean ± SEM (** $p<0.01$, and ***$p < 0.001$; $n \geq 3$).

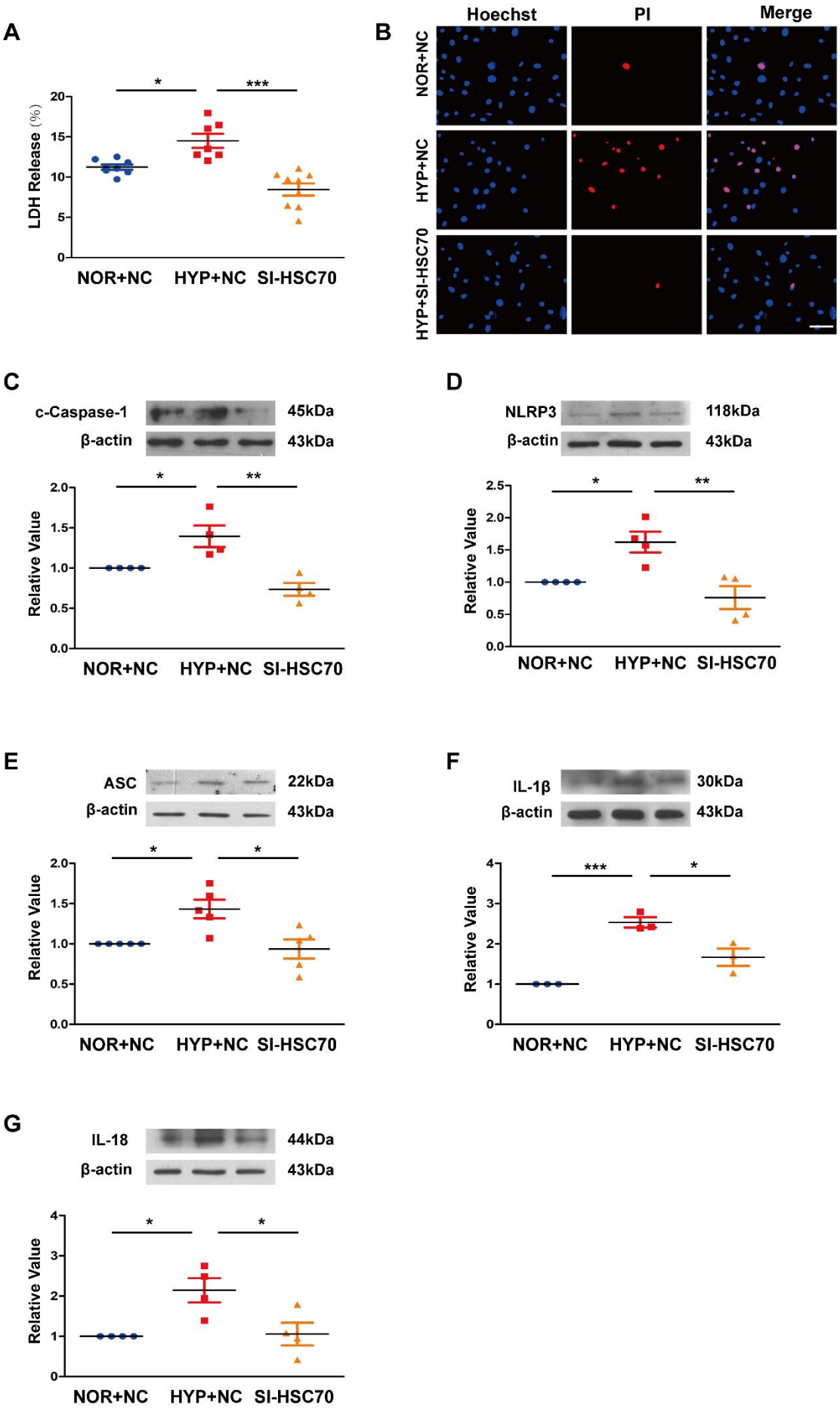
A
LDH Release (%)
NOR+NC
HYP+NC
SI-HSC70
B
Hoechst
PI
Merge
NOR+NC
HYP+NC
HYP+SI-HSC70
C
c-Caspase-1
45kDa
β-actin
43kDa
Relative Value
D
NLRP3
118kDa
β-actin
43kDa
Relative Value
E
ASC
22kDa
β-actin
43kDa
Relative Value
F
IL-1β
30kDa
β-actin
43kDa
Relative Value
G
IL-18
44kDa
β-actin
43kDa
Relative Value

Supplemental figure 7. Interfering with HSC70 inhibits hypoxia-induced pyroptosis of PASMCs. (A) LDH release assay in hypoxic and normoxic PASMCs transfected with SI-HSC70, or SI-NC. (B) PI staining in hypoxic and normoxic PASMCs transfected with SI-HSC70, or SI-NC (Scale bar = 50 μm). (C-G) WB analysis of (C) c-Caspase-1 (D) NLRP3, (E) ASC, (F) IL-1β and (G) IL-18 in hypoxic and normoxic PASMCs transfected with SI-HSC70, or SI-NC. All values are represented as the mean ± SEM (*p<0.05, **p<0.01, and ***p< 0.001; n ≥ 3). NOR, normoxia; HYP, hypoxia.

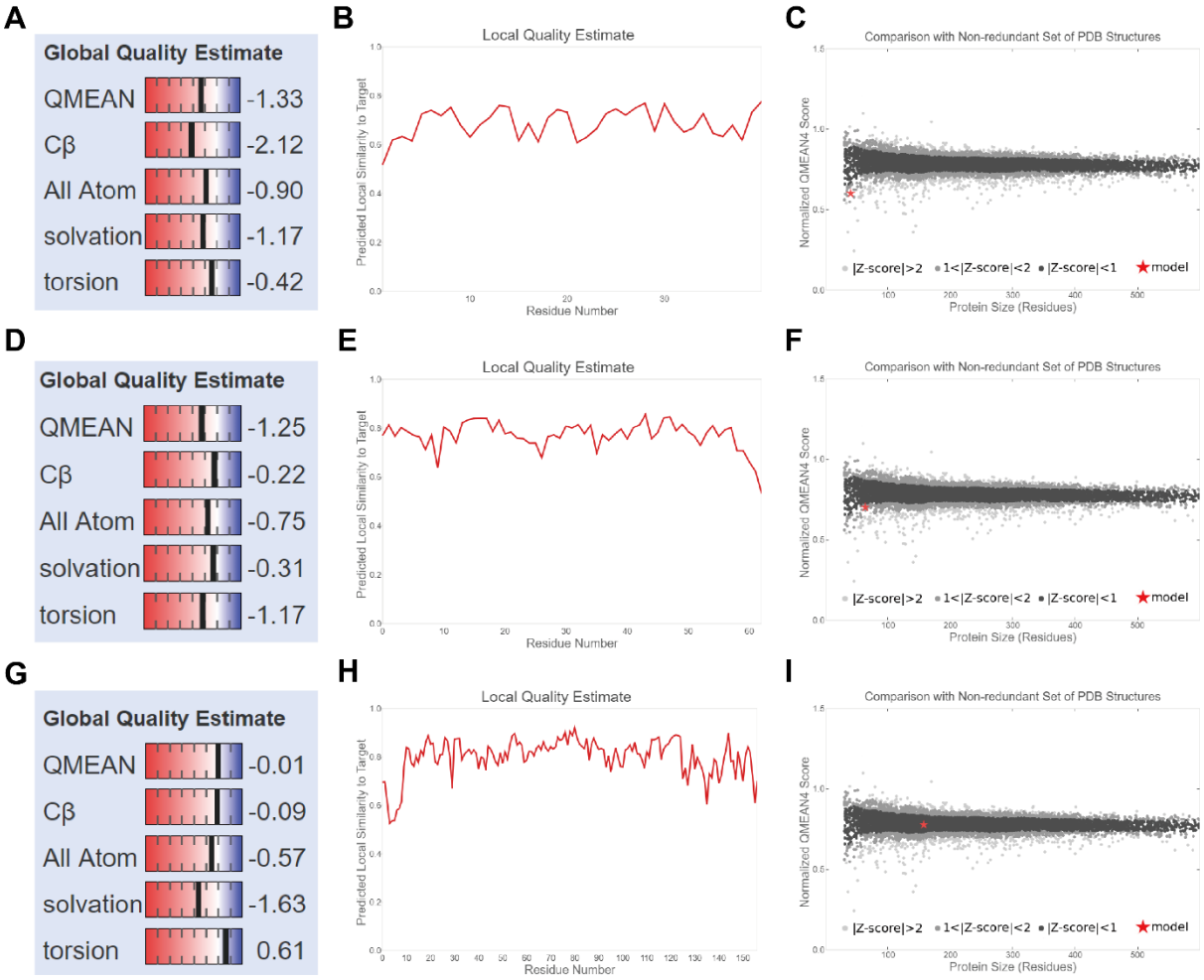

Supplemental Figure 8. Global and local quality estimates and standardized QMEAN4 scores of the RPS4XL domains using a structure model. (A) Global quality (B) Local quality estimate (C) Standardized QMEAN4 scores for the RPS4XL 1–41 aa domain. The (D) global quality, (E) local quality estimate, and (F) standardized QMEAN4 scores for the RPS4XL 42–104 aa domain. The (G) global quality, (H) local quality estimate, and (I) standardized QMEAN4 scores for the RPS4XL 105–262 aa domain.

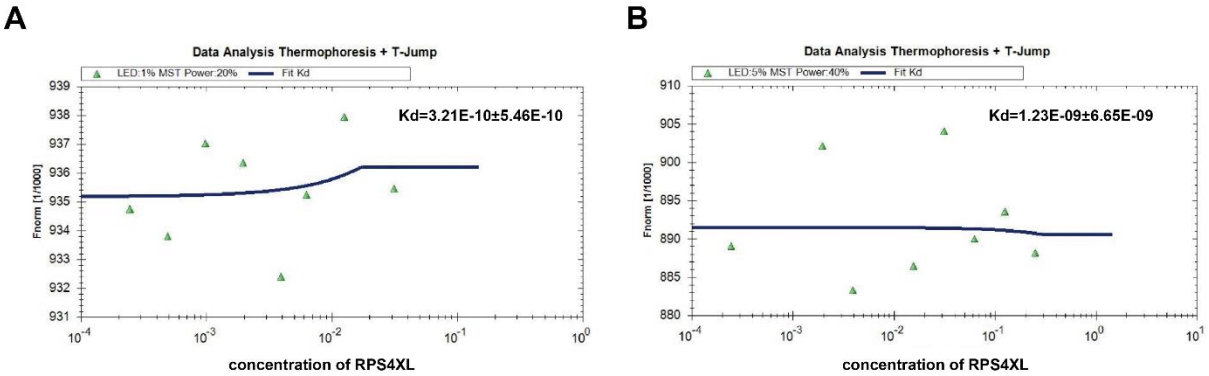

Supplemental Figure 9. RPS4XL does not bind to the 394–509 aa or 510–646 aa HSC70 domains. Microscale thermophoresis of the HSC70 (A) 394–509 aa and (B) 510–646 aa domains when combined different concentrations of RPS4XL.

A

```
Name:  sp_P63017_HSP7C_MOUSE  Length:  393
MSKGPAVGIDLGTTYSCVGVFQHGKVEIIANDQGNRTTPSYVAFTDTERLIGDAAKNQVAMNPTNTVFDAKRLIGRRFDD      80
AVVQSDMKHWPFMVVNDAGRPKVQVEYKGETKSFYPEEVSSMVLTKMKEIAEAYLGKTVTNAVVTVPAYFNDSQRQATKD     160
AGTIAGLNVLRIINEPTAAAIAYGLDKKVGAERNVLIFDLGGGTFDVSILTIEDGIFEVKSTAGDTHLGGEDFDNRMVNH     240
FIAEFKRKHKKDISENKRAVRRLRTACERAKRTLSSSTQASIEIDSLYEGIDFYTSITRARFEELNADLFRGTLDPVEKA     320
LRDAKLDKSQIHDIVLVGGSTRIPKIQKLLQDFFNGKELNKSINPDEAVAYGAAVQAAILSGDKSENVQDLLL
.................................N.........................N..................      80
.....................................................................N.........     160
................................................................................     240
................................................................................     320
....................................N.............................. .             400
```

B

```
(Threshold=0.5)
--------------------------------------------------------------------------------
SeqName      Position  Potential   Jury    N-Glyc
                                agreement result
--------------------------------------------------------------------------------
sp_P63017_HSP7C_MOUSE   35 NRTT   0.6463     (8/9)   +
sp_P63017_HSP7C_MOUSE   62 NPTN   0.7830     (9/9)   !!!  WARNING: PRO X1.
sp_P63017_HSP7C_MOUSE  151 NDSQ   0.5564     (8/9)   +
sp_P63017_HSP7C_MOUSE  360 NKSI   0.5788     (8/9)   +
```

C

```
Name:  sp_P63017_H              Length:  393
MSKGPAVGIDLGTTYSCVGVFQHGKVEIIANDQGNRTTPSYVAFTDTERLIGDAAKNQVAMNPTNTVFDAKRLIGRRFDD
AVVQSDMKHWPFMVVNDAGRPKVQVEYKGETKSFYPEEVSSMVLTKMKEIAEAYLGKTVTNAVVTVPAYFNDSQRQATKD
AGTIAGLNVLRIINEPTAAAIAYGLDKKVGAERNVLIFDLGGGTFDVSILTIEDGIFEVKSTAGDTHLGGEDFDNRMVNH
FIAEFKRKHKKDISENKRAVRRLRTACERAKRTLSSSTQASIEIDSLYEGIDFYTSITRARFEELNADLFRGTLDPVEKA
LRDAKLDKSQIHDIVLVGGSTRIPKIQKLLQDFFNGKELNKSINPDEAVAYGAAVQAAILSGDKSENVQDLLL
................................................................................
................................................................................
................................................................................
................................................................................
................................................................................
```

D

Name	S/T	Pos	G-score	I-score	Y/N	Comment
sp_P63017_H	S	2	0.422	0.386	.	-
sp_P63017_H	T	13	0.283	0.027	.	-
sp_P63017_H	T	14	0.273	0.071	.	-
sp_P63017_H	S	16	0.164	0.026	.	-
sp_P63017_H	T	37	0.293	0.031	.	-
sp_P63017_H	T	38	0.283	0.192	.	-
sp_P63017_H	S	40	0.216	0.021	.	-
sp_P63017_H	T	45	0.318	0.053	.	-
sp_P63017_H	T	47	0.295	0.053	.	-
sp_P63017_H	T	64	0.201	0.146	.	-
sp_P63017_H	T	66	0.210	0.021	.	-
sp_P63017_H	S	85	0.109	0.055	.	-
sp_P63017_H	T	111	0.335	0.032	.	-
sp_P63017_H	S	113	0.225	0.022	.	-
sp_P63017_H	S	120	0.206	0.075	.	-
sp_P63017_H	S	121	0.188	0.073	.	-
sp_P63017_H	T	125	0.314	0.056	.	-
sp_P63017_H	T	138	0.270	0.020	.	-
sp_P63017_H	T	140	0.262	0.079	.	-
sp_P63017_H	T	145	0.292	0.198	.	-
sp_P63017_H	S	153	0.259	0.019	.	-
sp_P63017_H	T	158	0.283	0.077	.	-
sp_P63017_H	T	163	0.265	0.147	.	-
sp_P63017_H	T	177	0.230	0.043	.	-
sp_P63017_H	T	204	0.190	0.049	.	-
sp_P63017_H	S	208	0.127	0.021	.	-
sp_P63017_H	T	211	0.244	0.073	.	-
sp_P63017_H	S	221	0.160	0.056	.	-
sp_P63017_H	T	222	0.255	0.278	.	-
sp_P63017_H	T	226	0.237	0.023	.	-
sp_P63017_H	S	254	0.117	0.054	.	-
sp_P63017_H	T	265	0.281	0.045	.	-
sp_P63017_H	T	273	0.319	0.031	.	-
sp_P63017_H	S	275	0.219	0.060	.	-
sp_P63017_H	S	276	0.214	0.024	.	-
sp_P63017_H	S	277	0.216	0.020	.	-
sp_P63017_H	T	278	0.294	0.038	.	-
sp_P63017_H	S	281	0.223	0.082	.	-
sp_P63017_H	S	286	0.196	0.023	.	-
sp_P63017_H	T	295	0.190	0.062	.	-
sp_P63017_H	S	296	0.117	0.041	.	-
sp_P63017_H	T	298	0.177	0.049	.	-
sp_P63017_H	T	313	0.186	0.029	.	-
sp_P63017_H	S	329	0.174	0.019	.	-
sp_P63017_H	S	340	0.096	0.052	.	-
sp_P63017_H	T	341	0.150	0.061	.	-
sp_P63017_H	S	362	0.121	0.325	.	-
sp_P63017_H	S	381	0.155	0.070	.	-
sp_P63017_H	S	385	0.203	0.059	.	-

Supplemental Figure 10. Prediction of N-glycosylation and O-glycosylation sites in the 1–393 aa domain of HSC70. (A and B) Bioinformatics prediction of N-glycosylation site in the 1–393aa domain of HSC70 using NetNGlyc. (C and D) Bioinformatics prediction of O-glycosylation site in 1–393 aa domain of HSC70 using DictyOGlyc.

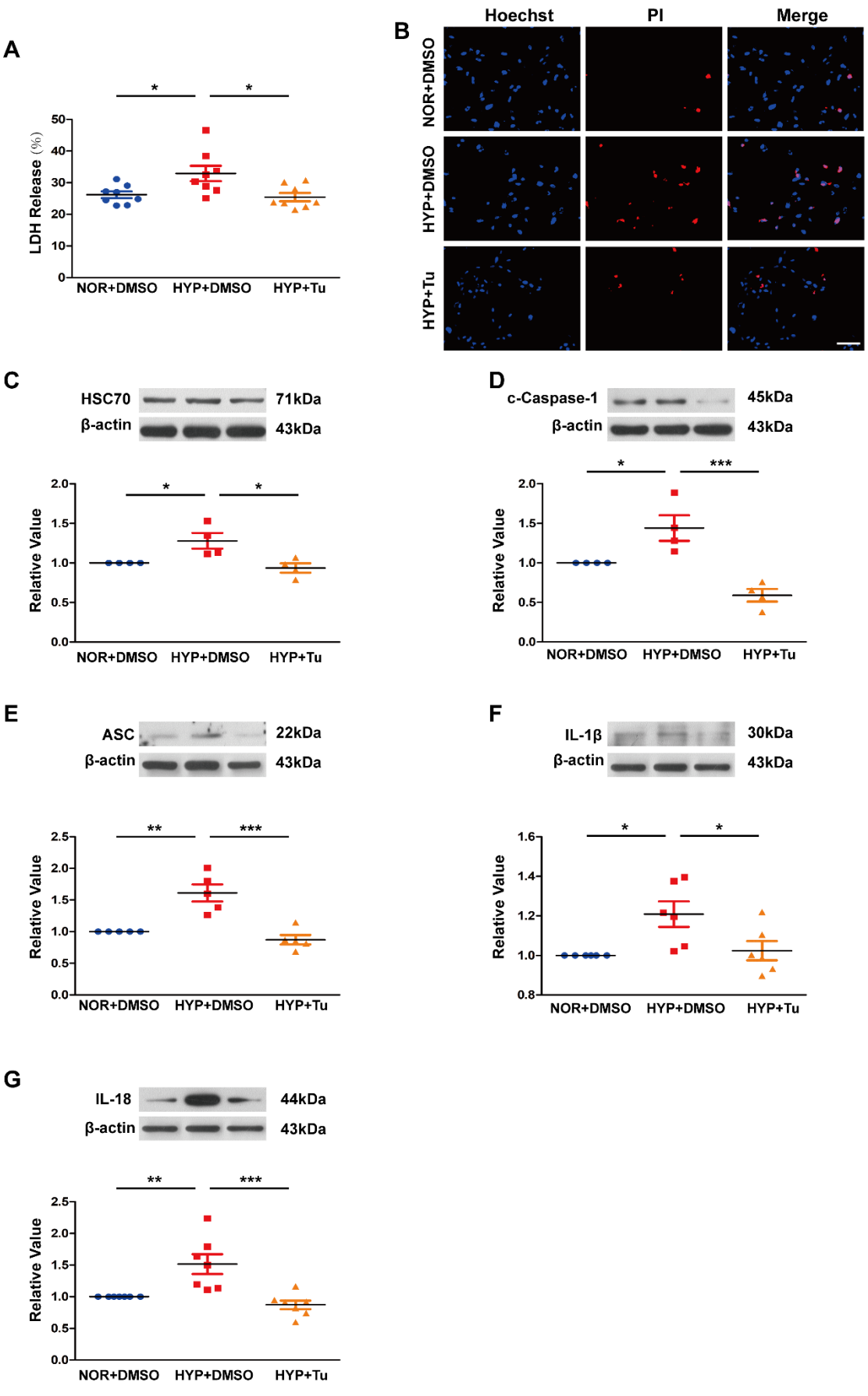
A
LDH Release (%)
NOR+DMSO
HYP+DMSO
HYP+Tu
B
Hoechst
PI
Merge
C
HSC70
β-actin
71kDa
43kDa
Relative Value
D
c-Caspase-1
45kDa
E
ASC
22kDa
F
IL-1β
30kDa
G
IL-18
44kDa

Supplemental Figure 11. The glycosylation inhibitor tunicamycin inhibits hypoxia-induced pyroptosis in PASMCs. (A) LDH release in PASMCs treated with 1 μg/ml tunicamycin under hypoxia. (B) PI staining in PASMCs treated with 1 μg/ml tunicamycin under hypoxia (Scale bar = 50 μm). (C-G) Western blotting analysis of (C) HSC70, (D) c-caspase-1, (E) ASC, (F) IL-1β, and (G) IL-18 in PASMCs treated with 1 μg/ml tunicamycin under hypoxia. All values are represented as the mean ± SEM (*p<0.05, **p<0.01, and ***p< 0.001; n ≥ 3). NOR, normoxia; HYP, hypoxia; Tu; tunicamycin.